

Central Lancashire Online Knowledge (CLOK)

Title	Electroformation of Particulate Emulsions Using Lamellar and Nonlamellar Lipid Self-Assemblies
Type	Article
URL	https://clock.uclan.ac.uk/id/eprint/40174/
DOI	https://doi.org/10.1021/acs.langmuir.1c02721
Date	2021
Citation	Bailey, Lauren Frances, Prabhakaran, Jayaschandran Vavolil, Vishwapathi, Vinod and Kulkarni, Chandrashekhhar Vishwanath (2021) Electroformation of Particulate Emulsions Using Lamellar and Nonlamellar Lipid Self-Assemblies. <i>Langmuir</i> , 37 (49). pp. 14527-14539. ISSN 0743-7463
Creators	Bailey, Lauren Frances, Prabhakaran, Jayaschandran Vavolil, Vishwapathi, Vinod and Kulkarni, Chandrashekhhar Vishwanath

It is advisable to refer to the publisher's version if you intend to cite from the work.
<https://doi.org/10.1021/acs.langmuir.1c02721>

For information about Research at UCLan please go to <http://www.uclan.ac.uk/research/>

All outputs in CLOK are protected by Intellectual Property Rights law, including Copyright law. Copyright, IPR and Moral Rights for the works on this site are retained by the individual authors and/or other copyright owners. Terms and conditions for use of this material are defined in the <http://clock.uclan.ac.uk/policies/>

Electroformation of Particulate Emulsions using Lamellar and Non-lamellar Lipid Self-assemblies

Lauren F. Bailey^a, Jayachandran Vavolil Prabhakaran^b Vinod Kumar Vishwapathi^{a,c}, and Chandrashekhar V. Kulkarni^{a}*

^aCentre for Smart Materials, School of Natural Sciences, University of Central Lancashire, Preston, PR1 2HE, United Kingdom

^bApplied Biology Section, Department of Applied Sciences, University of Technology and Applied Sciences, PO Box 74, Al-Khuwair, Postal Code 133, Muscat, Sultanate of Oman

^cSchool of Pharmacy and Biomedical Sciences, University of Central Lancashire, Preston, PR1 2HE, United Kingdom.

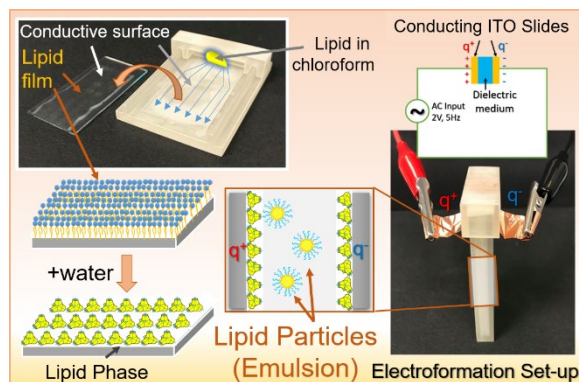
*Corresponding Author: E-mail: cvkulkarni@uclan.ac.uk, Tel: +44-1772-89-4339, Fax: +44-1772-89-4981.

Abstract

We report on the development of an electroformation technique for the preparation of particulate (particle-based) emulsions. These oil-in-water (here, lipid phase acts as an ‘oil’) emulsion were prepared using non-lamellar lipid phases. Such emulsion particles offer high hydrophobic volumes compared to conventional lipid particles based on lamellar phases (vesicles/liposomes). In addition, tortuous internal nanostructure contributes through greater surface area per volume of lipid particles allowing an enhanced loading of payloads. An electroformation method makes use of a capacitor formed from two indium tin oxide (ITO) coated conductive glass surfaces separated by a dielectric aqueous medium. This capacitor set-up is enclosed in a custom-designed 3-D printed unit. Lipid molecules, deposited on conductive surfaces, self-assemble into a nanostructure in the presence of aqueous medium, which when subjected to an AC electric field forms nano-and/or micro-particles. Optical microscopy, dynamic light scattering (DLS), and small angle X-ray scattering (SAXS) techniques were employed for micro-and nanostructural analyses of electroformed particles. With this method, it is possible to produce particulate emulsions at a very low (e.g. 0.0005 wt% or 0.5 mg/ml) lipid concentrations. We demonstrate an applicability of electroformation method for drug delivery by preparing lipid particles with curcumin, which is highly important but water-insoluble medicinal compound. As the method employs gentle conditions, it is potentially non-invasive for the delivery of delicate biomolecules and certain drugs, which are prone to decomposition or

denaturation due to high thermo-mechanical energy input and/or non-aqueous solvents required for existing methods.

Graphical Abstract



Keywords: Electroformation, particulate emulsion, non-lamellar lipid phases, lipid self-assembly, ITO coating, non-invasive drug delivery

1. Introduction

At low temperatures and/or hydrations, a majority of lipids tend to form lamellar phases (e.g. crystalline (L_C), gel (L_β or L_β^*), inverted ribbon (P_δ), or fluid lamellar (L_α)) (Figure 1a).¹ Upon hydration, a few lipids form non-lamellar phases (Figure 1a) which may include bicontinuous cubic $Im3m$, $Pn3m$ and $Ia3d$ phases. The complex architecture, in these phases, is formed by draping continuous a lipid bilayer on primitive (P), double diamond (D) and gyroid (G) type infinite periodic minimal surfaces (IPMS)², respectively. The 3-dimensionally organized bilayer separates continuous aqueous channels on its either sides.³ The sponge phase (L_3)⁴, formed by some lipids, particularly lipid mixtures, is also ‘bicontinuous’ in nature but its bilayer is disorganized on the contrary to highly ordered cubic nanostructures. Such a tortuous arrangement attributes to a very large lipid/water interfacial area (as high as 400 m²/g)⁵ in these bicontinuous lipid phases, beneficial for enhanced loading of active ingredients. Hexagonal (H_2) and fluid isotropic (L_2) are other commonly observed non-lamellar lipid phases (Figure 1a)⁶.

Other than aforementioned thermodynamically equilibrium lyotropic phases, lipids also form kinetically stabilized architectures including vesicles/liposomes (usually from lamellar phases) and hierarchically organized structures, for instance, water-in-oil (W/O)⁷ and oil-in-water (O/W) emulsions from non-lamellar phases (Figure 1b)³. Note that, the ‘oil phase’ in this case is formed of liquid crystalline lipid phase/s and/or unstructured lipid ensembles. If the internal self-assembly of

lipid particles is of ‘cubic’ type nanostructure, the O/W emulsions are called ‘cubosomes’,⁸ whereas if the internal self-assembly is ‘hexagonal’ (H_2) phase, the particles are regarded as hexosomes,⁹ and so on.³ Cubosomes and hexosomes are more popular but other particles namely lamellarsomes,¹⁰ spongisomes¹¹ and particles of inverse micelles¹² were also prepared by the kinetic stabilization of lamellar, sponge (L_3) and fluid isotropic (L_2) phases, respectively. A group of researchers has formulated a smart term to describe these colloidal particles with a single word, “isasomes”, i.e. ‘internally self-assembled *somes*’ (meaning bodies or particles).¹² These particles are generally of micron or submicron size but their internal architecture is always ‘nanostructured’, with at least one dimension of ‘nanoscale’ length. Note that, solid lipid nanoparticles (SLN) and, an advanced version, nanostructured lipid carriers (NLC)¹³ differ from isasomes in terms of an internal phase, which is usually none other than lamellar or fluid isotropic.

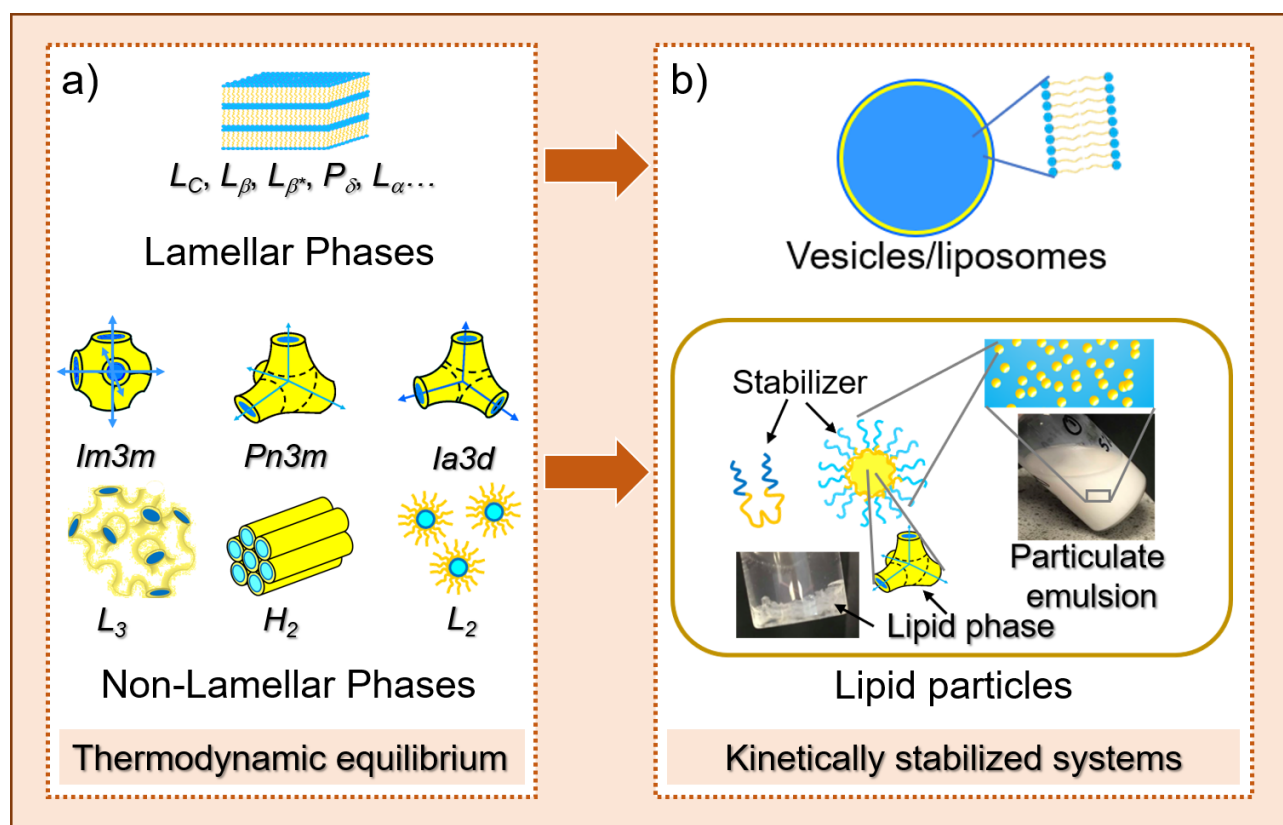


Figure 1. Lipid Phases and Derived Systems. a) Commonly observed self-assembled nanostructures formed by lipid molecules: lamellar phase whose polymorphs can be crystalline (L_C), gel (L_β or L_{β^*}), inverted ribbon (P_δ), fluid lamellar (L_α), etc.; and non-lamellar phases including bicontinuous cubic $Im3m$, $Pn3m$ and $Ia3d$, bicontinuous sponge phase (L_3), inverse hexagonal (H_2) and fluid isotropic (inverse spherical micelles) (L_2). b) Kinetically stable vesicles/liposomes are formed by molecules that can form lamellar phases. Giant sized vesicles (≥ 1000 nm) usually exhibit locally planar lipid bilayers. Non-lamellar phases are dispersed into oil-in-water particulate emulsions, which constitute self-assembled nanostructures at the cores of lipid particles (as an oil phase). Large hydrophobic volumes exhibited by these particles is favourable for loading of water-insoluble payloads as compared to vesicles.

Larsson¹⁴ mentioned the term ‘cubosomes’ in his review published in 1989, but Gustafsson et al.⁸ reported the first preparation of cubosomes in 1996 using micro-fluidization and sonication techniques, which are the main methods employed on laboratory scale even today. These top-down approaches are based on the fragmentation of a pre-formed viscous cubic phase by subjecting it to mechanical high-energy input such as vigorous mixing, high pressure, high shear and/or strong sonic waves at raised temperatures of about 40-60 °C.¹⁵ Spicer et al. developed a bottom-up approach in 2001, enabling the industrial scale production of cubosomes, and more importantly evading the use of very high-energy inputs as well as high temperatures.¹⁶⁻¹⁷ This method utilizes ethanol in the form of ‘hydrotrope’ to enhance the solubility of insoluble lipid molecules. However, hydrotropes tend to show adverse effects on the stability and/or activity of certain biomolecules; for instance, some proteins denature due to an interaction with hydrotropes (e.g. with ethanol).¹⁸ A vast majority of proteins also denature at higher temperatures.¹⁹ Structures and activities of nucleic acids,²⁰ vitamins²¹ as well as of some drugs²² are also disturbed at raised temperatures.

Another low-energy method based on the solubilization of lipids in water-immiscible solvent, supported by an evaporation of other volatile solvent was developed, but this method requires ultrasonication; moreover involved solvents may not be suitable for several sensitive payloads²³. Therefore, a method addressing the aforementioned concerns would be highly suited for *in situ* encapsulation of various ‘delicate’ payloads. To this end, Kim et al. developed an ultra-chilled (<4 °C) indirect sonication method²⁴ based on cup horn geometry which effectively reduces the power subjected to the sample while the chilling controls the raising temperature. An experimental approach was similar to the commonly used thin film hydration method to prepare liposomes.²⁵ Microfluidics technology, explored by the same and other research groups, also provides mild conditions as demonstrated by successful loading of various molecules including nucleic acids.²⁶⁻²⁸ Not only cubosomes but also hexosomes were prepared by this method.²⁷ In addition, the method offers several advantages, including short production times, control over particle size and size distribution, and continuous and low-cost production. Nevertheless, microfluidics approach involves the use of ethanol,²⁶⁻²⁸ which is not compatible with a broad range of delicate payloads and hence their *in-situ* encapsulation.¹⁸

A few researchers were able to avoid harsh treatments of temperature and sonication by loading the cubosomes after their preparation.²⁹ However, post-preparation loading of cubosomes may not always be successful according to our work on the encapsulation of fullerenes, which could be only loaded during the preparation of cubosomes; the ones added after their preparation resulted into a strong sedimentation.³⁰ Therefore, any novel method, including an electroformation (reported in this

work), providing mild preparation conditions is highly desirable for non-invasive delivery of sensitive payloads.

We report a novel method to fabricate lipid particles using non-lamellar lipid phases, which does not entail harsh conditions, namely, high temperatures and high-energy input. This method is a systematic modification of an electroformation technique employed by Angelova et al. for the preparation of lipid vesicles (liposomes).³¹ The main principle of the electroformation technique is the electric field-driven swelling of lipid films deposited on electrode wires or indium tin oxide (ITO) conducting surfaces (coated onto glass slides) in the presence of water. Although this method was first used in 1986 (for the preparation of vesicles),³¹ and has been deeply investigated thereafter,³²⁻³⁵ it was never explored for the preparation of lipid particles using non-lamellar lipid self-assemblies. This could be attributed to the distinct mechanistic principles behind the structural stability of vesicles and nanostructured lipid particles. Vesicles are formed of single or multiple lipid bilayers enclosing an aqueous medium; the bilayers are arranged in such a way that lipid head groups face hydrophilic (e.g. aqueous) solvent on either sides; achieving kinetic stabilization of vesicular structures.³⁶ However, O/W particulate lipid emulsions require interfacial agents to induce the structural stability, as otherwise, the particles potentially formed by electroformation method will inevitably undergo an aggregation.⁸

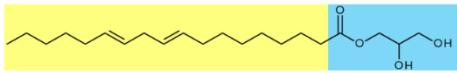
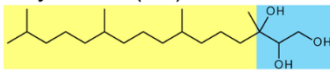
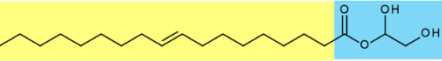
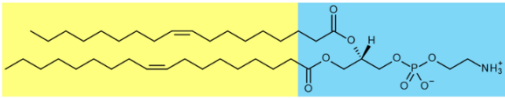

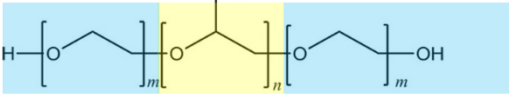
Lipids	Self-assembled Nanostructures (in Water)
Dimodan-U/J (DU) 	$L_C, L_\alpha, Ia3d, \text{Pn}3m, H_2, L_2$
Phytantriol (PT) 	$L_\alpha, Ia3d, \text{Pn}3m, H_2, L_2$
Monoelaidin (ME) 	$L_{C1}, L_\beta, L_{\beta^*}, L_\alpha, Ia3d, Pn3m, Im3m, L_2$
1,2-dioleoyl-sn-glycero-3-phosphoethanolamine (DOPE) 	$L_C, L_\beta, P_\delta, L_\alpha, H_2$
1,2-dioleoyl-sn-glycero-3-phosphocholine (DOPC) 	L_C, L_α
Pluronic® F127 	An interfacial stabilizer – forms type 1 micelles

Figure 2. Chemical structures of lipids and a stabilizer (Pluronic®F127) used to prepare O/W emulsions (nanostructured lipid particles). Hydrophobic and hydrophilic parts of the molecules are indicated with yellow and blue colours, respectively. Self-assembled nanostructures formed by corresponding amphiphiles (DU,³⁷ PT,³⁸ ME,¹ DOPE,³⁹ DOPC⁴⁰ and F127⁴¹) in water are listed on right side, while the ones present under current study conditions are highlighted yellow.

In this work, we tested several fluids including pure water, and aqueous solutions of a) glucose, b) sorbitol and c) a stabilizing agent, Pluronic® F127 ([PEO]_m-[PPO]_n-[PEO]_m block-copolymer). We observed that the presence of stabilizing molecules is a very important factor in the electroformation of particulate emulsions. In order to check the versatility of the electroformation method, we studied a range of lipids (Figure 2) that form non-lamellar as well as lamellar self-assemblies, including phospholipids: 1,2-dioleoyl-sn-glycero-3-phosphoethanolamine (DOPE) and 1,2-dioleoyl-sn-glycero-3-phosphocholine (DOPC), monoglycerides: Dimodan®-U/J (DU) and monoelaidin (ME), and phytantriol (PT). Electroformed emulsions were analysed for their morphological features using scattering and microscopic techniques.

2. Experimental Section

2.1. Materials

The main lipid used in this study was Dimodan®-U/J (DU), supplied by Danisco-DuPont (Denmark). DU (Figure 2) is a distilled glyceride, consisting of 96 % monoglycerides, 4 % diglycerides and free fatty acids. The hydrophobic region of DU primarily contains C₁₈ chains as the two primary monoglyceride elements are linoleate (62%) and oleate (25%). Other lipids, monoelaidin (ME) and phytantriol (PT) were purchased from Tokyo Chemical Industry UK Ltd., whereas 1,2-dioleoyl-sn-glycero-3-phosphoethanolamine (DOPE) and 1,2-dioleoyl-sn-glycero-3-phosphocholine (DOPC) were purchased from Avanti Polar Lipids (Figure 2). Chloroform and Pluronic® F127 (now on F127) were purchased from Sigma-Aldrich (Dorset, UK) (Figure 2). Curcumin (≥90% pure) was purchased from Cambridge Bioscience Ltd. The DU and F127 were stored below 4 °C, whereas other lipids were stored at approximately -20 °C. All compounds were used without further purification. The water used throughout the study was purified using Barnstead Nanopure system, Thermo Scientific (USA).

2.2. Preparation of particulate emulsions via ultra-sonication

Molten DU (500 mg) in 20 ml scintillation vial (from VWR, UK) was topped with 9.5 g of 0.5% F127 solution, resulting in a 50 mg/ml lipid in a stabilizer (F127) solution i.e. 5 wt% lipid in F127 solution. The mixture containing viscous cubic phase (Figure 1d iii) was ultra-sonicated for a total pulse time of 5 minutes (pulse of 1 second at the delay of 1 second) using Sonics & Materials Vibra-Cell VCX-750 Ultrasonic Processor (Jencons Scientific Ltd., UK) at constant amplitude of 30%. This method yields approximately 10 ml emulsion that appears as a milky-white fluid (Figure 1d iii). This emulsion was stable at room temperature for several months after preparation.

2.3. Preparation of particulate emulsions via electroformation

Electroformation of particulate emulsions involved three steps, first, creating a thin film of lipid molecules onto conductive surfaces, second, formation of self-assembled lipid nanostructure by soaking the lipid film in water and third, emulsification under an electric field. The Custom-designed ‘lipid spreading unit’ and ‘electroformation chamber’ (Figure 3), correspondingly employed for above steps, were obtained by 3-D printing additive technology.⁴² We have used such prototypes for producing giant unilamellar vesicles (GUVs) required to prepare nanobilayers for hybrid nanopores and subsequent biomolecules’ translocation studies.⁴³

To make the thin film, DU (50 mg) was dissolved in 1 ml of chloroform, resulting in a 50 mg/ml lipid-chloroform solution. More solutions of DU (0.5 mg/ml, 1 mg/ml and 10 mg/ml) and of other

lipids (PT, ME, DOPE and DOPC) were prepared in this manner by solubilizing corresponding concentrations of lipids in the chloroform. An indium tin oxide (ITO)-coated glass slide (dimensions 25 mm x 50 mm x 1.1 mm; Visiontek Systems, Ltd., Chester, UK) was positioned into the slot of the lipid spreading unit (Figure 3a). The conductive layer of the ITO glass slide was identified with its typical resistance of 12-15 Ω using a Fluke 116 Digital HVAC Multimeter (Fluke Corporation, WA, USA). Using a micropipette, 10 μ l of the lipid solution was added onto one end of the ITO glass slide (placed in lipid spreading unit). This solution was carefully spread by sliding the top part of the lipid-spreading unit over the ITO slide (Figure 3a). During the solution spreading, the chloroform evaporates rapidly thereby creating a uniform thin lipid film on the ITO conductive layer (Figure 3a). Residual solvent (chloroform) was removed by vacuum desiccation for 1 hour. This process was repeated for another ITO glass slide.

Lipid-deposited ITO slides were submerged in excess water for 10 minutes to ensure the formation of desired self-assembled lipid nanostructures (Figure 3b). The time of 10 minutes was found enough for maximum water absorption by lipid films (supporting Figure S1). Subsequently, the excess water was drained by holding the ITO slides vertically for a few seconds. Water immersion step may well be omitted as the desired phase can form in an aqueous media contained in the electroformation chamber even without pre-soaking. However, this step could become crucial for encapsulation of payloads during the formation of the lipid phase itself. Conducting adhesive copper tape (0.035 mm thick, 10 mm wide, RS Components, UK) was fixed on the conductive sides of both slides (to aid electric connections). ITO slides were then placed in an electroformation chamber, with the conducting surfaces facing each other (Figure 3c). Both slides were separated by

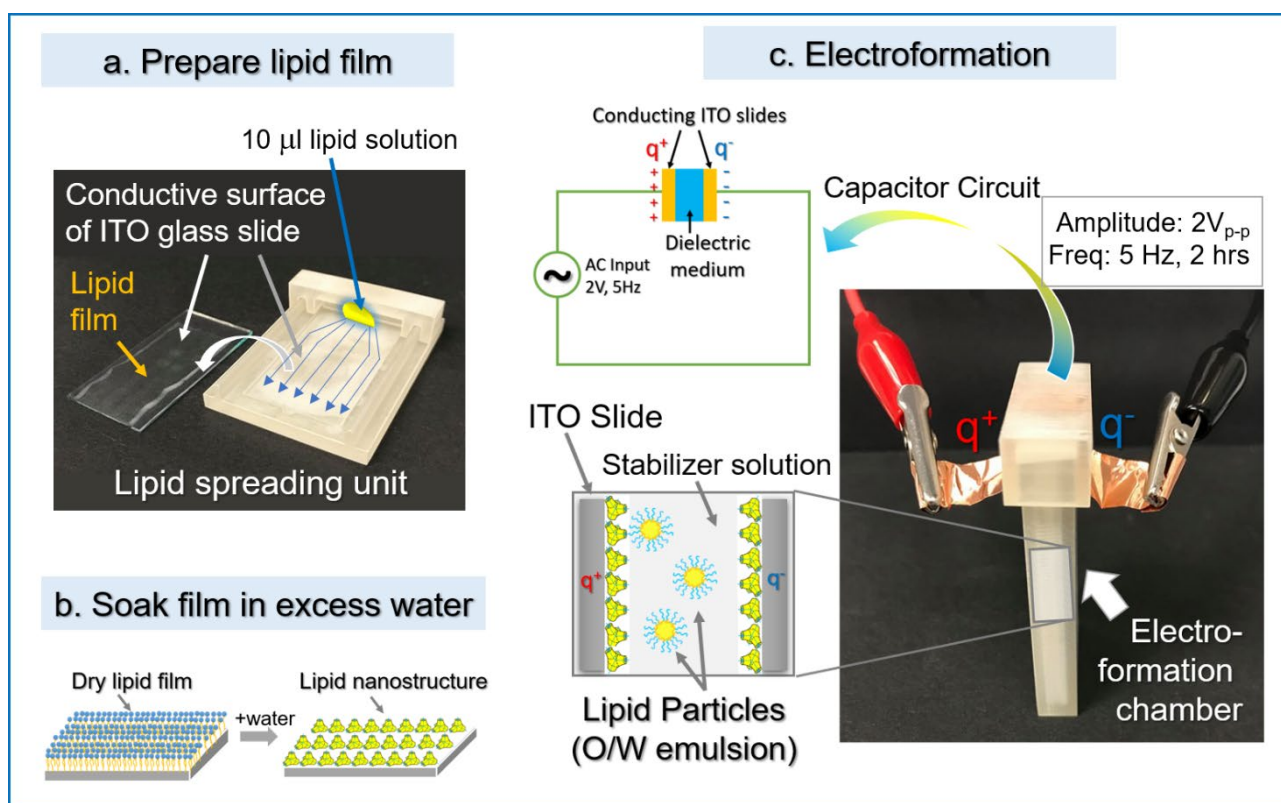


Figure 3. Electroformation set-up. a) The Thin lipid film on a conductive ITO slide is fabricated by spreading a lipid solution in chloroform (using a lipid-spreading unit), followed by chloroform evaporation. b) The lipid phase is then formed by immersing a lipid-coated ITO slide in water. c) To aid electric connections, conducting copper tape was affixed to an ITO slide. Two such slides are then placed in an electroformation chamber followed by the addition of stabilizer solution. Upon application of an electric field, opposite charges (q^+ and q^-) are adopted by two conducting surfaces forming a capacitor (formed by two conducting ITO slides separated by a dielectric aqueous medium) which facilitates the formation of nanostructured lipid particles.

a 1 mm gap generated by purposefully designed 1 mm thick protrusions in the chamber.⁴³ ITO slides were then connected to the Aim-TTi TG320 Function Generator (RS Components, UK) via conducting copper tapes. 2 ml of 0.5 % F127 solution was added into the chamber. This assembly is now ready to serve as a capacitor.

An alternating current (AC) with amplitude of $2V_{p-p}$ and sine-wave frequency of 5 Hz was applied for two hours (unless specified) at room temperature using the function generator. After two hours, the particulate emulsion from the electroformation chamber was carefully collected using a 1 ml plastic syringe and hypodermic needle, followed by transfer into 2 ml Eppendorf tubes in three aliquots collected from top, middle and bottom of the electroformation chamber.

2.4. Particle size analysis

The mean particle size and the size distribution of lipid particles in particulate emulsions were determined using dynamic light scattering (DLS) technique. A Zetasizer Nano ZS instrument (Malvern Panalytical Ltd., UK) operated at 25 °C was used for this purpose. Emulsion samples were collected from the bottom, middle and top of the electroformation chamber (Figure 3). Electroformed emulsions were diluted with a dilution factor of 1:5, whereas a dilution factor of 1:20 was used for ultra-sonicated samples, all were made up to 1 ml with pure H₂O. The shapes, and again the size of lipid particles were analysed using a Nikon Eclipse E200-LED optical microscope (Nikon Instruments, UK) at a magnification of 40x.

2.5. Identification of self-assembled nanostructures using small angle X-ray scattering (SAXS)

Liquid crystalline bulk phases formed from mixtures of 40 wt/wt% lipids and 0.5% aqueous solution of F127 were identified using small angle X-ray scattering (SAXS). A SAXSpace instrument (Anton Paar, Graz, Austria) was used for this purpose; the details of which were provided earlier.⁴⁴ Briefly, the sealed-tube Cu-anode generator cooled by closed water circuit was operated at 40 kV and 50 mA. The camera (Anton Paar, Graz, Austria) with line-focus employs Cu-K_α radiation at a wavelength (λ) of 1.54 Å. Acquired scattering patterns were corrected with respect to the primary beam using the SAXStreat software (Anton Paar, Graz, Austria) whereas SAXSQuant software (Anton Paar, Graz, Austria) was used for all other standard corrections. Bulk liquid crystalline phases were studied using a paste cell sample holder and fluid (particulate emulsion) samples were studied using a 1 mm diameter capillary holder (Anton Paar, Graz, Austria). All measurements were performed at 25±1°C unless otherwise mentioned. Several SAXS measurements were also performed using a SAXSLAB Ganesha 300XL instrument. A typical exposure of 7200 seconds was used for emulsions loaded in 1.5 mm capillaries measured at 10±2 °C. Patterns from empty and water-filled cells were utilized for standard background corrections. Characteristic peak ratios calculated using Millar indices (hkl) were employed to distinguish lipid phases as follows: $\sqrt{2}$, $\sqrt{3}$, $\sqrt{4}$, $\sqrt{6}$, $\sqrt{8}$ for *Pn3m* Phase, $\sqrt{2}$, $\sqrt{4}$, $\sqrt{6}$ for *Im3m* phase, 1, $\sqrt{3}$, $\sqrt{4}$ for hexagonal (*H*₂) phase and 1, 2, 3, 4 for lamellar phases. Sponge phase (*L*₃) and inverse fluid micellar phase (*L*₂) were detected from characteristic broad peaks⁴⁵.

For acquiring descent scattering patterns with SAXS, approximately 10 ml electroformed DU dispersions (collected from five electroformation experiments) were concentrated to 0.5 ml as follows: DU samples were added to Amicon™ Ultra-4 Centrifugal Filter Units with Ultracel-3 membranes (Sigma-Aldrich, Dorset, UK) and centrifuged at 4000 rpm for 40 minutes (Jouan B4i

Centrifuge, Jencons Scientific Ltd., UK). This protocol was not followed for bulk phases and an emulsion produced by ultrasonication, as they scattered well enough for distinguishing pertinent nanostructures.

A few SAXS measurements were also performed on I22 Beamline at the synchrotron facility in Diamond Light Source, Oxford, UK. Typical parameters were as follows: Beam energy - 12.4 keV, wavelength 1 Å, sample to detector distance- 5719.2 mm and the data were collected as a stack of 100 x 0.1 s frames, which were subsequently averaged. Water-filled capillary was used for background subtraction. Measurements were performed at room temperature using high-throughput capillary rack.

3. Results and Discussion

An electroformation method, described in section 2.3, yields approximately 2 ml solution of lipid particles (O/W emulsion), which remained stable for at least two months at room temperature. This solution had 0.5 mg/ml of lipid in aqueous solution (0.05 wt% lipid in F127 solution).

3.1. Micro and nanoscale morphology of lipid particles

Visual properties of solutions namely, translucent or turbid confirm the formation of lipid particles, at the first instance (Figure 5). Second level of confirmation was attained from the images generated using an optical microscope (Figure 4 a, b); based on their size and morphological features, at least two types of lipid particle populations were clearly visible.

Smaller lipid particles (indicated by white arrows in Figure 4 a, b) appear denser but the larger ones (indicated by black arrows) appear less dense (more swollen). Particles visible in optical micrographs range between 200 nm and 2 µm in size. According to dynamic light scattering (DLS) analyses, a majority (82.8%) of lipid particles formed by the commonly used ultrasonication method⁸ were 277 ± 122 nm whereas electroformed particles were three times bigger (832 ± 302 nm) as depicted in Figure 4c. A minimal amount of lipid aggregation, in the form of larger lumps (≥ 5 µm), was seen in both methods. There was an additional peak around 100 nm for electroformed lipid particles, which can be understood to be F127 micelles, as the F127 content (20 mg) was 10 times higher than lipid content (2 mg) in the electroformation chamber. Pure F127 in excess water is known to form normal (*type I*) spherical micelles at room temperature whose size ranges between 34 Å -114 Å.⁴¹

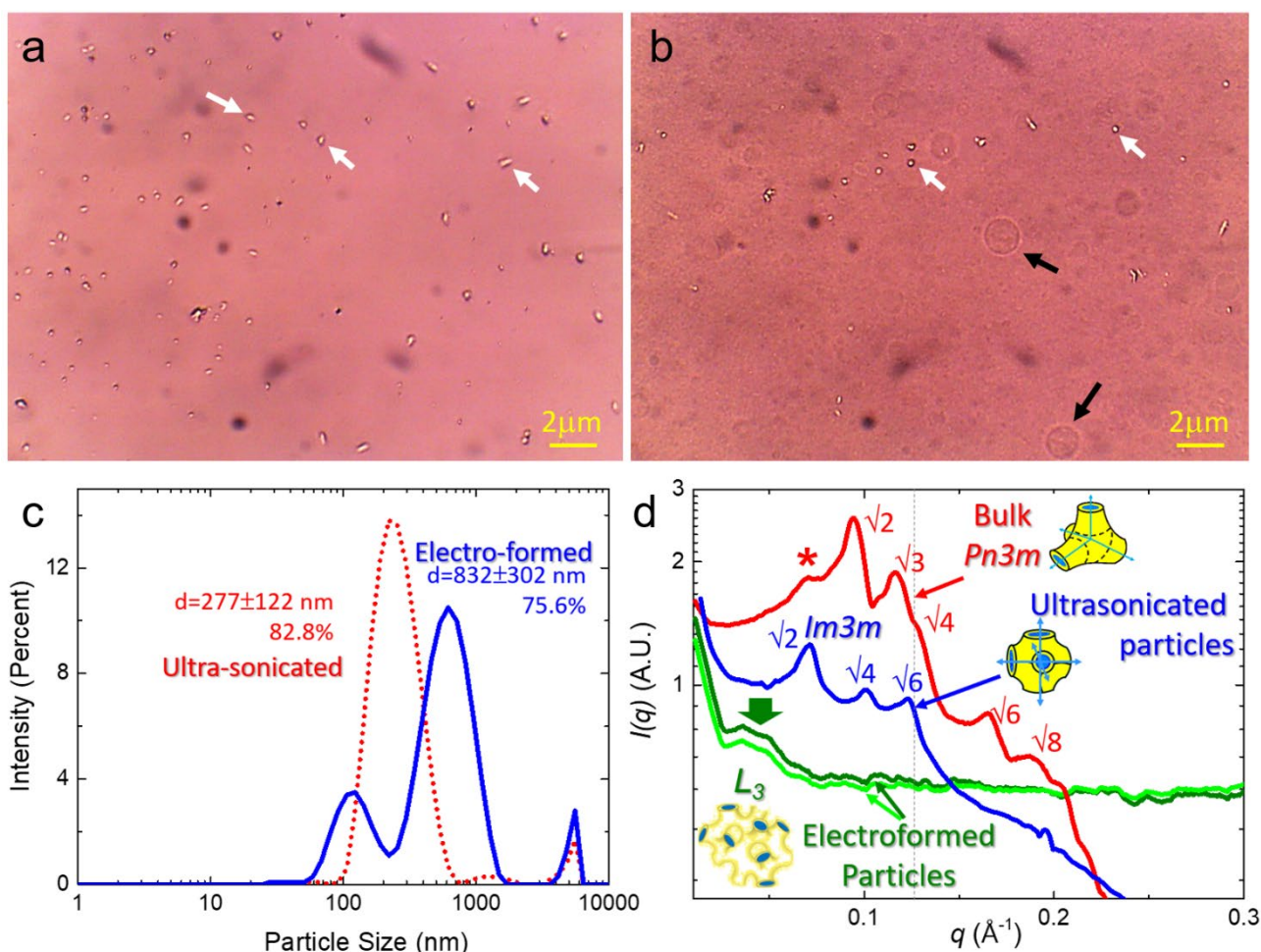


Figure 4. Microstructural and nanostructural analysis of lipid particles. Optical micrographs of electroformed lipid particles prepared from a) 1 mg/ml and b) 50 mg/ml DU in 0.5 % F127 solution. White arrows indicate small-sized lipid particles (~300-500 nm) whereas black arrows specify larger lipid particles (> 1 μm). c) Particle size distribution of ultrasonicated (red dots) and electroformed (blue solid line) nanostructured lipid particles formed from 50 mg/ml DU in 0.5 % F127 solution measured by dynamic light scattering technique. The percentage numbers indicate relative abundance of the particles having diameter 'd' (in nm). d) In bulk state DU forms $Pn3m$ cubic phase (red curve) in excess water, which upon interaction with F127 stabilizer transforms into $Im3m$ cubic phase (blue curve) situated in the core of lipid particles (called cubosomes due to cubic phase interior). Characteristic peak ratios $\sqrt{2}$, $\sqrt{3}$, $\sqrt{4}$, $\sqrt{6}$, $\sqrt{8}$ for $Pn3m$ and $\sqrt{2}$, $\sqrt{4}$, $\sqrt{6}$ for $Im3m$ distinguish the cubic phases for bulk and ultrasonicated samples. In case of electroformed particles, the internal nanostructure transforms into sponge (L_3) phase typified by broad peak around $q = 0.04 \text{ \AA}^{-1}$ (designated by downward block arrow). Schematic diagrams of parts of $Pn3m$, $Im3m$ and L_3 unit cells are shown near corresponding SAXS patterns.

Small angle X-ray scattering (SAXS) analyses provided details of nanoscale morphology of lipid phases in bulk and within dispersed particles (Figure 4d). DU⁴⁶ forms $Pn3m$ cubic phase (peak ratios $\sqrt{2}$, $\sqrt{3}$, $\sqrt{4}$, $\sqrt{6}$, $\sqrt{8}$) in excess water with lattice parameter of 89.5 \AA , but due to the presence of F127 (0.5 wt% aqueous solution) it was increased to 92.6 \AA . In case of ultrasonicated lipid particles, an interaction of DU with F127 is known to cause phase transition into $Im3m$ cubic phase⁴⁷ (peak ratios $\sqrt{2}$, $\sqrt{4}$, $\sqrt{6}$) with a lattice parameter of 123 \AA (Figure 4d). A peak represented

by $\sqrt{2}$ (shown by * in [Figure 4d](#)) is visible in bulk DU revealing the coexistence of *Im3m* phase with *Pn3m* phase (red curve). However, electroformed emulsions (represented by green and dark green curves in [Figure 4d](#)) showed signals from sponge phase, instead of cubic phases, which could be confirmed from a broad peak in the low q region ($q = 0.04 \text{ \AA}^{-1}$) (indicated by downward block arrow).⁴⁸ This phase transition is a result of excessive presence of stabilizer molecules compared to the lipid itself. Aqueous solution in the electroformation chamber contained 0.5 % F127, meaning it had ~20 mg F127 whereas the total weight of lipid on two ITO slides together was less than 2 mg (for 1 mg/ml lipid sample). Owing to this, the resulting nanostructure was strongly influenced by self-assembling properties of F127. Pure F127 in water generally forms normal micelles (L_1) at room temperature⁴¹ but when mixed with lipids, it competes for the curvature of the resulting phases.^{8, 49} Pluronic F127 and closely related polyethylene glycols generally induce sponge phase formation in cubic phase forming lipids.^{4, 50-51} Sponge phase containing electroformed lipid particles are called spongisomes or spongosomes.^{3, 52}

3.2. Effect and optimization of experimental parameters

Electroformation protocol was optimized by carefully altering various parameters including type of aqueous media (with/without stabilizer), temperature of an electroformation chamber, time of electroformation, type and concentration of lipids and concentration of a stabilizer:

a) Effect of solvent medium: Several solutions namely, sorbitol in water, glucose in water and pure water were tested for the preparation of particulate emulsions, but it was found that stable lipid particles form only in the presence of stabilizer F127 solution, otherwise strong aggregation was observed at both room temperature (20 °C) and physiological temperature (37 °C).

b) Effect of temperature: Electroformation was conducted at 20 °C and 37 °C; particles were successfully prepared at both temperatures; however, there was no significant difference in the size or size distribution of particles between those prepared at physiological temperature and at room temperature. The pattern of particle size distribution was reproducible (recorded for four samples at 20 °C and three samples at 37 °C of 50 mg/ml lipid concentration, as shown in [supporting Figure S2](#)).

c) Effect of lipid concentration: Electroformation was employed successfully to produce nanostructured lipid particles from 0.5 mg/ml, 1 mg/ml, 5 mg/ml, 10 mg/ml, 25 mg/ml and highest concentration, of 50 mg/ml (an equivalent concentration was used for the preparation of O/W emulsion via ultrasonication) lipid in 0.5 % F127 solution in water. Owing to the large height of the electroformation chamber (compared to its width and thickness) and the density difference between lipid and water, lipid particles/aggregates were found to disperse unevenly at various levels

(heights) of the chamber, as elucidated by DLS patterns in Figure 5. Density of DU (1.07083 g/cm^3 at 25°C) is greater than water (0.99707 g/cm^3 at 25°C), therefore large DU aggregates (of size $\sim 4\text{--}5 \mu\text{m}$) were sedimented at the bottom, additionally the particle size distribution from them was quite broad (e.g. for 25 mg/ml and 50 mg/ml samples in Figure 5a). Particle size distribution was relatively narrow for particles at top and medium levels, particularly for low lipid containing samples (0.5 mg/ml, 1 mg/ml and 10 mg/ml). Large particles (of size $\sim 4\text{--}5 \mu\text{m}$) were found at all levels for high lipid containing samples ($>10 \text{ mg/ml}$). All samples were stable against phase separation for at least 2 months, which can be confirmed from pictures of homogeneous emulsions in Figure 5a.

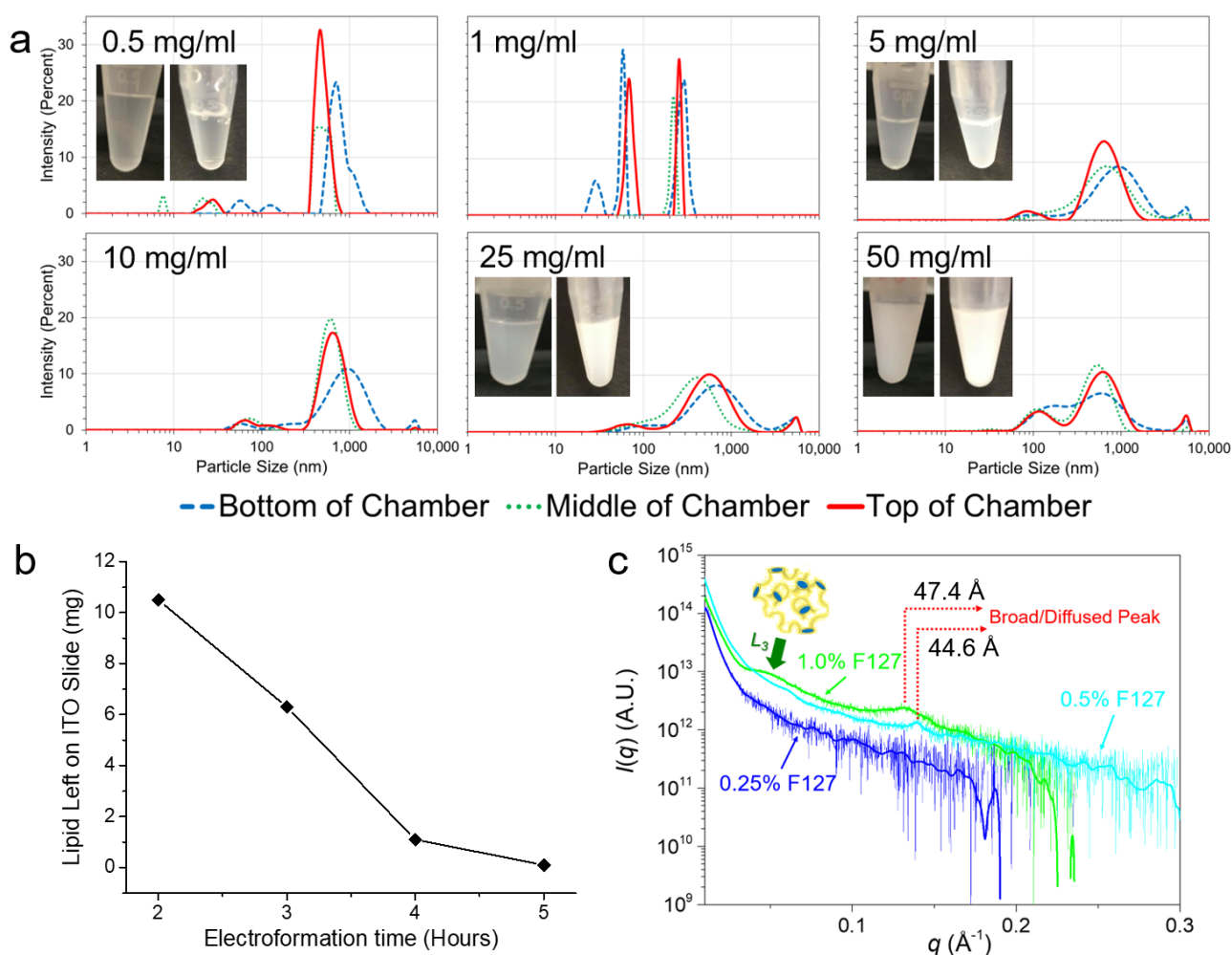


Figure 5. a) Variation of lipid concentration: Particle size distribution broadened for high lipid containing samples when the lipid (DU) concentration was varied from 0.5 mg/ml to 50 mg/ml in 2 ml of 0.5% F127 solution. Pictures of Eppendorf tubes depict visibly homogeneous and stable dispersions of lipid particles, captured immediately after preparation (L) and after two months (R); slight aggregation happening over two months is visible from an increase in turbidity of originally translucent dispersions; however all samples were stable against phase separation. b) Weight of lipid left on ITO slide (on Y-axis) after 2, 3, 4 and 5 hours of experimental time for 50 mg/ml lipid concentration. c) SAXS patterns from nanostructured lipid particles prepared for various F127 stabilizer concentrations for 1 mg/ml lipid concentration. The latter affects the internal nanostructure of lipid particles, which is converted into sponge (L_3) and

inverse micellar (L_2) phases indicated by broad peaks. Characteristic distance for L_2 phase increased with F127 concentration from 44.6 to 47.4 Å. Samples show low scattering even at synchrotron source because they were made from low lipid contents (1 mg/ml i.e. 0.1 % lipid).

d] Effect of electroformation time: For 25 mg/ml and 50 mg/ml concentrations, significant amounts of lipid remained on the ITO slides despite of the high number density of lipid particles; suggesting that the electroformation technique works better for lower lipid concentrations where almost all of the coated lipid was utilized for preparation of nanostructured lipid particles. An extension of experimental time from 2 hours to 5 hours aided in reducing the lipid content remaining on the ITO slides (Figure 5b) (photos and particle size distribution with experiment time are shown in supporting Figure S3). However, 2 hours was an optimum time for preparation of lipid particles using lower (≤ 10 mg/ml) lipid concentrations as in this case the amount of lipid left after 2 hrs electroformation was negligible.

e] Effect of stabilizer concentration: The concentration of Pluronic® F127 stabilizer for all electroformation and ultrasonication studies was 0.5 wt% in water. Two other concentrations 0.25 % and 1.0 % were also investigated to determine the influence of the stabilizer concentration on the nanostructure of lipid particles. Visibly the electroformed samples looked similar, but the small angle X-ray scattering (SAXS) patterns recorded at synchrotron source were able to identify the differences (Figure 5c). Broad peaks (around $q = 0.04 \text{ Å}^{-1}$ and $0.13\text{-}0.14 \text{ Å}^{-1}$) in Figure 5c elucidate that the original cubic phase nanostructure (Figure 4d) was converted into other phase/s. This is because as the proportion with respect to lipids increases, pluronic surfactants, including F127, are known to induce phase transitions from $Pn3m$ to $Im3m$ to Sponge (L_3) phase or sometimes to inverse micellar L_2 phase (also called emulsified microemulsion¹² when in dispersed form).^{48-49, 53-54} 1 mg/ml lipid was used to prepare lipid particles in 2 ml of 0.25 %, 0.5 % and 1.0 % F127; an approximate proportion was as follows: 2 mg lipid per 5, 10 and 20 mg of F127, respectively (density of F127 is 1.018 g/cm^3). Such high F127 contents affect the ‘type of lipid nanostructure’ formed.

For DU, the region around $q = 0.13\text{-}0.14 \text{ Å}^{-1}$ (Figure 5c) typically belongs to fluid lamellar phase (L_α);³⁷ the d -spacing of 47.4 Å for lipid particles containing 1.0 % F127 and 44.6 Å was determined for particles containing 0.5 % F127. The coexistence or inter-transitions of unilamellar and/or multilamellar vesicles (underlying lamellar phases) is quite common when non-lamellar phases are emulsified into particulate emulsions, as discussed here.⁵⁴⁻⁵⁶ However, the broadness of these peaks indicates the formation or co-existence of inverse micellar (L_2) phase (Figure 5c). Thus, electroformed particles of DU were a mixture of spongisomes (L_3 in the interiors) and emulsified microemulsions (L_2 in the interiors). The latter was not detected on lab based SAXS machine (see

Figure 4d) but was only identified using high energy synchrotron source SAXS instrument (as in Figure 5c).

3.3. Extending the electroformation technique for other lipids

In order to verify the usefulness and versatility of electroformation technique for the preparation of lipid particles from other lipids, we tested PT, ME, DOPE and DOPC (chemical structures are shown in Figure 2). These lipids differ in their chemical structures determining their phase behaviour in excess water condition at room temperature, a majority of which form non-lamellar phases: PT contains three hydroxyl groups in the head group and three methyl side groups attached to an alkyl chain in the tail region; forms *Pn3m* cubic phase.³⁸ ME is C₁₈ monoglyceride consisting 'trans' unsaturation at (9:10) position; forms lamellar phase at room temperature, but sometimes coexist with *Im3m* cubic phase, which occurs at a little higher temperature.^{1, 57} DOPE and DOPC contain two oleyl chains, each with an unsaturation at (9:10) position; head groups, however, are comprised of ethanolamine and choline groups respectively. DOPE and DOPC, correspondingly, form hexagonal⁵⁸ and lamellar⁴⁰ phases in excess water.

In presence of dilute F127 (used to stabilize lipid particles) the phase behaviour can be slightly different than in excess water conditions, discussed above. Figure 6a displays the SAXS patterns of various lipid phases formed in bulk states (non-dispersed systems). Similar to DU, the PT also forms *Pn3m* cubic phase in dilute F127 aqueous solution (Figure 6a); however, the lattice parameter (69.7 Å) is smaller with respect to that of DU due to small lipid length. ME also forms cubic (*Im3m* and *Pn3m*) phases in dilute F127 aqueous solution,⁵⁶ but at room temperature (20 °C) it exists in lamellar state (Figure 6a) with lattice parameter of 49.8 Å. DOPE and DOPC form hexagonal phase (Figure 6a) and lamellar (Figure 6a) phase respectively, with lattice parameters of 63.8 Å and 60.9 Å. Upon electroformation, the internal nanostructure of PT and ME was found to transform into sponge phase (indicated by broad peaks around $q = 0.04 \text{ Å}^{-1}$ in Figure 6b) whereas DOPE and DOPC did not show clear indication of any nanostructure. The form factor from particles was visible for PT and ME (indicated by * in Figure 6b). The scattering from these electroformed particles was very low because they were prepared using very low lipid content (1 mg/ml lipid). Similar to DU, in all these cases, the F127 concentration was much excess (10 mg) compared to lipids (2 mg), hence the nanostructures were strongly dominated by F127. SAXS patterns from electroformed O/W emulsions of PT, ME, DOPE and DOPC are shown in Figure 6b.

Particles of 200-500 nm size were formed from PT (Figure 6c) whereas ME forms particles (diameter 200-300 nm) as well as rod-like structures, with rod lengths as long as 2 µm (supporting Figure S4b). DOPE (Figure 6c) and DOPC (Figure 6c) primarily formed sub-micron sized particles.

Optical micrographs of electroformed particles from PT, ME, DOPE and DOPC are shown in supporting Figure S4.

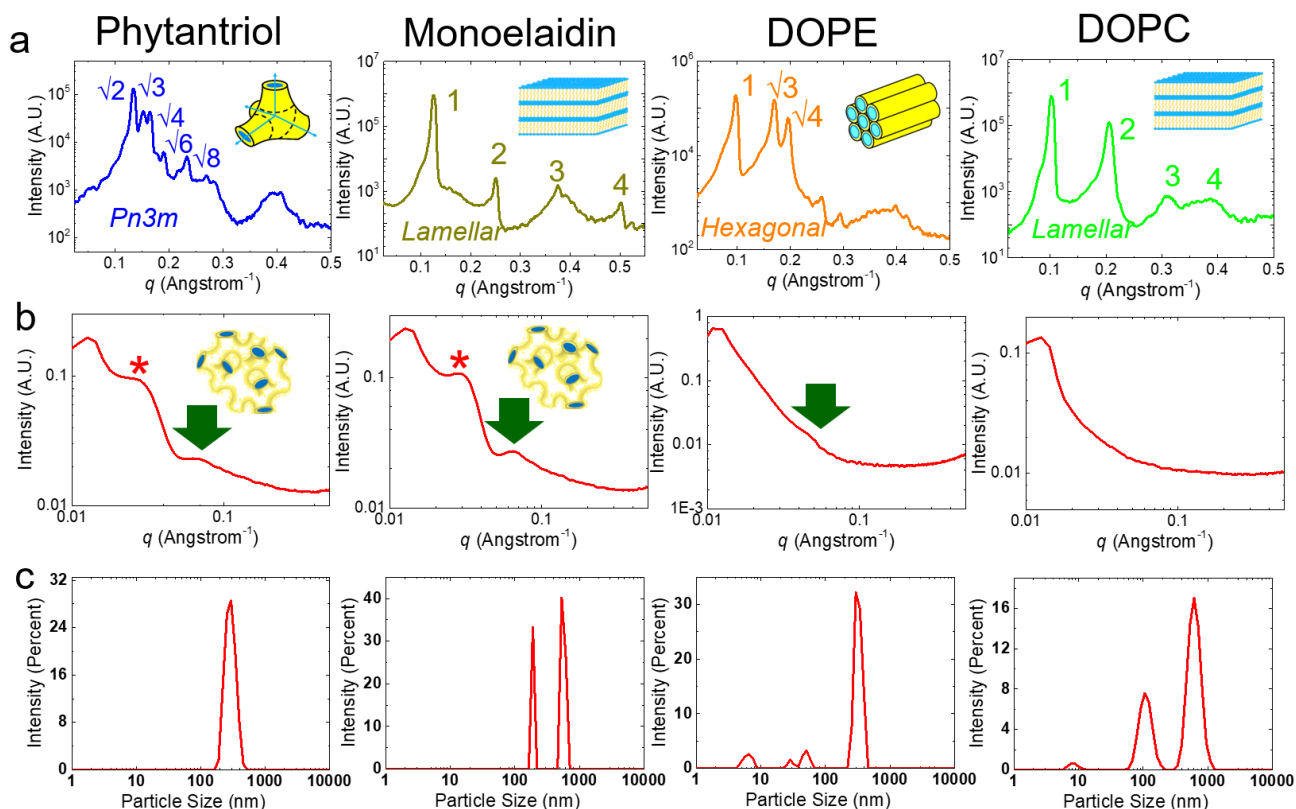


Figure 6. Structural analysis of lipid particles prepared from various lipids. a) SAXS patterns of PT, ME, DOPE and DOPC in bulk state indicating cubic $Pn3m$, Lamellar, H_2 and lamellar phases (with corresponding peak ratios), respectively, formed in 0.5 % F127 solution. b) SAXS patterns of electroformed particle dispersions. Broad peaks (downward block arrows) for PT and ME dispersions indicate the formation of sponge phase, whereas another peak at low q (indicated by *) illustrates the form factor from particles. A small shoulder around $q = 0.04 \text{ \AA}^{-1}$ is visible for DOPE, but no detectable peak is available for DOPC. However, the particle size distribution in c) confirms the formation of lipid particles.

It was a general observation that pure lipids, PT, ME, DOPE and DOPC, formed a higher number of particles when compared to DU (a commercial lipid containing a mixture of monoglycerides, in addition to the presence of some diglycerides). Moreover, the particles from pure lipids appeared to be more monodispersed and exhibited submicron sizes (optical micrographs in supporting Figure S4).

3.4. Understanding the mechanism of electroformation of lipid particles prepared from non-lamellar lipid phases

The mechanism behind the formation of lipid particles from non-lamellar lipid phases is understood to be similar to the proposed mechanism³¹ of electroformation of vesicles; however, the kinetic stability is attained differently. In case of vesicles, two-dimensional (2-D) lipid bilayers, deposited

onto the ITO slides, swell in the presence of an aqueous solution, roll into spherical particles, and consequently detach from the conductive surface.³¹ Energy required for the separation of bilayers and their bending is provided by an external electric field.³¹ Vesicle formation requires optimum proportion between structured parts (in the form of bilayers) and holes or defects in the lipid film on an ITO slide. Electrostatic and osmotic forces help in overcoming van der Waals attractions between bilayers - for thick lipid layers, while lipid-solid surface interactions - in case of very thin films.³¹ These events result into bending and fusion of bilayers to form vesicles. Finally, the kinetic stability of vesicles is ensured by the bilayer arrangement of lipid molecules minimizing the contact between hydrophobic tails and the hydrophilic aqueous phase.

In case of lipids that form non-lamellar phases, namely cubic and hexagonal, the lipid film itself has a nano-porous structure. Bicontinuous cubic phases, $Pn3m$ and $Im3m$, exhibit four- and six- aqueous channel junctions, respectively, formed by a draping continuous bilayer around Double Diamond (D) and Primitive (P) type minimal surfaces,⁶ whereas inverse hexagonal phase (H_2) is formed of long cylinders enclosing water channels. Thus, the required proportion between defects, in the form of pores, and bilayer regions is readily available within the lipid layer deposited on ITO slides. Furthermore, the bilayers are highly curved in contrast to planar lamellar phases (for vesicles), which are presumed to aid in further bending and fusion of lipid layers. Thus, upon application of an external electric field, the pre-formed cubic phase swells and detaches from the ITO slides to form internally structured particles. Stabilizer (pluronic F127) molecules present in an aqueous solution sterically stabilize an interface of electroformed particles to avoid their aggregation. The hydrophobic [PPO] block of F127 interacts with the hydrophobic surface and/or interior of the lipid particle while hydrophilic [PEO] blocks interact with water. Such stabilization can also be anticipated for lipid particles with lamellar (for ME and DOPC) and hexagonal (DOPE) internal nanostructures. This proposed mechanism, however, requires systematic verification through further studies.

3.5. Application for drug loading: Electroformation of lipid particles with curcumin

To demonstrate an applicability of electroformation method, we prepared lipid particles with a medicinal compound that is not soluble in water (solubility < 0.1 mg/ml at pH 7).⁵⁹ We chose curcumin for this purpose because it has characteristic yellow colour and it is an active ingredient of turmeric which exhibits prominent properties beneficial to the human health.⁶⁰ Lipid coated ITO slides (see section 2.3 for more details) were dipped in 5 ml suspension of curcumin in water (concentration of ~50 mg/ml) for about 10 minutes (Figure 7). Curcumin gets loaded into hydrated lipid phase (cubic $Pn3m$ phase) as depicted by typical yellow coloured lipid films (Figure 7c).

Curcumin-loaded lipid particles (Figure 7d) were then prepared by following an electroformation protocol described in section 2.3. Resulting particulate emulsion was stable (against phase separation) for more than 4 months (observation time) at room temperature.

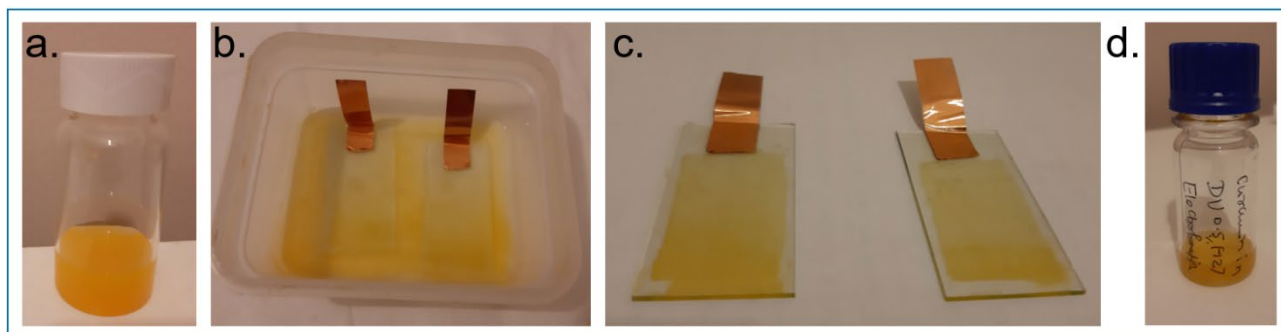


Figure 7. Electroformation of curcumin-loaded lipid particles: a) First a suspension of curcumin was prepared in water, which was then used to soak lipid films on ITO slides (b). As shown in c) both films turn yellow due to loading of curcumin in lipid phase. d) Electroformation using these films (in presence of 0.5% F127 solution) produces particulate emulsion with a typical yellow colour.

3.6. Advantages/limitations of an electroformation method for the preparation of lipid particles

Table 1 reviews an electroformation method, primarily, based on our observations.

Table 1. Advantages, limitations and potential solutions of electroformation technique for the preparation of self-assembled nanostructured lipid particles.

Advantages / important features of electroformation technique	
<ol style="list-style-type: none"> 1. No use of high energy 2. No use of non-aqueous solvent during electroformation 3. Works at room temperature as well as physiological temperature 4. Works with extremely low lipid concentrations (as low as 0.0005 wt% or 0.5 mg/ml); beneficial to prepare nanomolar formulations for biological and pharmaceutical studies 5. Works with lipids that form lamellar as well as non-lamellar liquid crystalline phases 6. Can produce submicron as well as micron sized particles 7. Easy and low-cost to set-up (for lab-scale production) 8. Potentially non-invasive for the delivery of sensitive biomolecules 9. <i>In-situ</i> loading of payloads possible 10. Nanostructure can be tuned by altering the composition of lipid and aqueous phases (for instance, mixture of lipids can be used instead of a single lipid or aqueous phase can be contained with the component/s that can alter the type and/or dimensions of nanostructures) 	
Limitation of electroformation technique	Potential solutions to address limitations

1. Produces polydisperse particles	1. With further optimization of conditions, it might be possible to get monodispersed particles; monodispersed particles can be also obtained by post-preparation treatment, e.g. extrusion using membranes ^{56, 61} of the desired pore size
2. Works only with low lipid contents (< 50 mg/ml)	2. By using less lipid, the method as such is cost-effective; for concentrations above 50 mg/ml lipid ⁶² other existing methods could be used.
3. Inhomogeneous dispersion of lipid particles in an electroformation chamber (particles float or sink depending on corresponding low or high density of lipid compared to aqueous medium)	3. Electroformed dispersion can be homogenized by gently shaking before their use; the design of electroformation chamber could be optimized to resolve this issue.
4. Large-scale production (currently) not feasible.	4. With further technological developments the large-scale production could be made feasible.

4. Conclusion

The Electroformation technique, developed in this report, was successfully implemented for the preparation of particulate emulsions using a range of lipids (Figure 6) forming lamellar as well as non-lamellar phases in excess water. Once a lipid is coated onto ITO slides (using a volatile solvent), the method only involves GRAS (generally recognized as safe) grade components, namely lipid, stabilizer and water. With a single experiment, it is possible to produce approximately 2 ml solution of lipid particles, which was stable at room temperature for two months of the study time. After this, a little aggregation was noted visibly, but the particles got dispersed again upon gentle shaking. It is anticipated that the internal structure of lipid particles does not change because the composition and parameters do not get altered following their preparation, and during the storage. The chain melting temperature, which is around 37 °C, does not have a strong influence on the formation and size distribution of lipid particles, as the method also works at 20 °C (Supporting Figure S2). Electroformation can be employed for a broad range of concentrations, with as low as 0.0005 wt% (or 0.5 mg/ml) lipid in F127 solution (Figure 5a), which has never been reported until now. It was possible to obtain lipid particles from as high as 50 mg/ml lipid concentration (maximum concentration used in current studies); however, it was recognized that a small amount of lipid still remained on the ITO slides within an experimental time of 2 hours. Extending the timescale of electroformation to 5 hours helped in utilizing the leftover lipid (supporting Figure S3), but we conclude that this is perhaps the upper limit of lipid concentration that can be used for

successful and efficient preparation of lipid particles, as it already contained some larger lipid aggregates (in the range of 5-10 μm and larger).

In the case of vesicles,³¹ the stabilization occurs via bilayer arrangement enabling the shielding of a hydrophobic chain region during electroformation. For electroformation of nanostructured lipid particles, an essential condition to be met is the availability of interfacial stabilizer that avoids inherent aggregation of lipid particles.

Electroformation involves gentle conditions for the preparation of O/W particulate lipid emulsions with an improved applicability, especially for *in-situ* encapsulation of active ingredients that are prone to undergo decomposition or denaturation due to harsh thermo-mechanical conditions. Loading of such sensitive ingredients can be done like the curcumin loading described in section 3.5 or by dissolving/suspending them in an aqueous solution in electroformation chamber. Although the process is driven by an electric field, it does not have the requirement of charged lipids. This is the first report on the preparation of oil-in-water emulsions containing lipid particles (in the form of oil phase) formed of non-lamellar lipids using an electroformation technique. Several challenges ([Table 1](#)) in terms of achieving homogeneity, mono-dispersity and desirable nanostructure as well as understanding the electroformation mechanism could be addressed through further research in this area. Nevertheless, the method opens up new avenues for the preparation and loading of nanostructured lipid particles for the delivery of an extensive range of active molecules.

Emerging applications in pharmaceutical and biotechnological disciplines demonstrate growing interests on internally self-assembled lipid particles, similar to the ones reported here. These particulate emulsions are highly suitable for insoluble drugs employable against major diseases, but more importantly, these particles have shown to accommodate an extensive range of molecules including agricultural actives, food ingredients, peptides, proteins, other lipids, dyes and stimuli-sensitive agents.^{29, 63-66} The efforts are now aligning towards predictable design and control of the structure-performance relationship of nanostructured lipid particles for desired applications, with particular emphasis on particle size, type and dimensions of internal nanostructures, composition of dispersed phase and the characteristic features required for the delivery of functional molecules.^{15, 65, 67} Development of novel techniques (for instance, ‘electroformation’ as presented here) and advancing the existing technologies for preparation and scaling-up of lipid particles are further areas gaining increased attention in recent years.

5. Supporting information

Supporting Information contains four [Figures \(S1 to S4\)](#) providing additional information on: weight change due to soaking of lipid film in water, effect of temperature on electroformation process and reproducibility, variation of electroformation time, and optical micrographs of electroformed particles prepared from various lipids.

6. Author Contributions

CVK planned and supervised the project; LFB and VKV performed experiments and analysed the data, JVP advised on optimization of parameters and potential applications, all authors wrote the manuscript.

7. Acknowledgements

We acknowledge Sana Sayed and Hifza Yaqoob for supporting with preliminary experiments. We would like to thank Prof Michael Rappolt and Dr Arwen Tyler from University of Leeds and Dr Annela Seddon from University of Bristol for providing access to SAXS instruments. Authors highly appreciate the beamtime (Proposal no. SM27882-1 on I22 Beamline) and the support provided by Dr Andy Smith and Dr Nick Terrill regarding SAXS experiments at the Diamond Light Source, Oxford, UK. LFB thanks to URIP (Summer Training Grant) at University of Central Lancashire.

8. References

1. Kulkarni, C. V., Nanostructural studies on monoelaidin-water systems at low temperatures. *Langmuir* **2011**, 27 (19), 11790-800.
2. Larsson, K., Periodic minimal surface structures of cubic phases formed by lipids and surfactants. *Journal of Colloid and Interface Science* **1986**, 113 (1), 299-300.
3. Kulkarni, C. V., Lipid crystallization: from self-assembly to hierarchical and biological ordering. *Nanoscale* **2012**, 4 (19), 5779-5791.
4. Ridell, A.; Ekelund, K.; Evertsson, H.; Engstrom, S., On the water content of the solvent/monoolein/water sponge (L3) phase. *Colloids and Surfaces A: Physicochemical and Engineering Aspects* **2003**, 228 (1-3), 17-24.
5. Lawrence, M. J., Surfactant systems: their use in drug delivery. *Chemical Society reviews* **1994**, 23 (6), 417-424.
6. Seddon, J. M., Structure of the inverted hexagonal (HII) phase, and non-lamellar phase transitions of lipids. *Biochimica et Biophysica Acta (BBA) - Reviews on Biomembranes* **1990**, 1031 (1), 1-69.
7. Kulkarni, C. V.; Mezzenga, R.; Glatter, O., Water-in-oil nanostructured emulsions: towards the structural hierarchy of liquid crystalline materials. *Soft Matter* **2010**, 6 (21), 5615-5624.
8. Gustafsson, J.; Ljusberg-Wahren, H.; Almgren, M.; Larsson, K., Cubic Lipid-Water Phase Dispersed into Submicron Particles. *Langmuir* **1996**, 12 (20), 4611-4613.

9. Nakano, M.; Teshigawara, T.; Sugita, A.; Leesajakul, W.; Taniguchi, A.; Kamo, T.; Matsuoka, H.; Handa, T., Dispersions of Liquid Crystalline Phases of the Monoolein/Oleic Acid/Pluronic F127 System. *Langmuir* **2002**, *18* (24), 9283-9288.
10. Battaglia, G.; Tomas, S.; Ryan, A. J., Lamellarsomes: metastable polymeric multilamellar aggregates. *Soft Matter* **2007**, *3* (4), 470-475.
11. Barauskas, J.; Johnsson, M.; Joabsson, F.; Tiberg, F., Cubic Phase Nanoparticles (Cubosome): Principles for Controlling Size, Structure, and Stability. *Langmuir* **2005**, *21* (6), 2569-2577.
12. Yaghmur, A.; de Campo, L.; Sagalowicz, L.; Leser, M. E.; Glatter, O., Emulsified Microemulsions and Oil-Containing Liquid Crystalline Phases. *Langmuir* **2005**, *21* (2), 569-577.
13. Muller, R. H.; Radtke, M.; Wissing, S. A., Nanostructured lipid matrices for improved microencapsulation of drugs. *Int J Pharm* **2002**, *242* (1-2), 121-8.
14. Larsson, K., Cubic lipid-water phases: structures and biomembrane aspects. *The journal of physical chemistry* **1989**, *93* (21), 7304-7314.
15. Wörle, G.; Drechsler, M.; Koch, M. H. J.; Siekmann, B.; Westesen, K.; Bunjes, H., Influence of composition and preparation parameters on the properties of aqueous monoolein dispersions. *International Journal of Pharmaceutics* **2007**, *329* (1), 150-157.
16. Spicer, P., Cubosome processing - Industrial nanoparticle technology development. *Chem Eng Res Des* **2005**, *83* (A11), 1283-1286.
17. Spicer, P. T.; Hayden, K. L.; Lynch, M. L.; Ofori-Boateng, A.; Burns, J. L., Novel Process for Producing Cubic Liquid Crystalline Nanoparticles (Cubosomes). *Langmuir* **2001**, *17* (19), 5748-5756.
18. Bull, H. B.; Breese, K., Interaction of alcohols with proteins. *Biopolymers* **1978**, *17* (9), 2121-2131.
19. Argos, P.; Rossmann, M. G.; Grau, U. M.; Zuber, H.; Frank, G.; Tratschin, J. D., Thermal stability and protein structure. *Biochemistry* **1979**, *18* (25), 5698-5703.
20. Driessen, R. P. C.; Sitters, G.; Laurens, N.; Moolenaar, G. F.; Wuite, G. J. L.; Goosen, N.; Dame, R. T., Effect of temperature on the intrinsic flexibility of DNA and its interaction with architectural proteins. *Biochemistry* **2014**, *53* (41), 6430-6438.
21. Frye, T. M. In *The performance of vitamins in multicomponent premixes.*, Proc. Roche Technical Symposium, Jefferson, Georgia, Jefferson, Georgia, 1994.
22. Censi, R.; Gigliobianco, M. R.; Casadidio, C.; Di Martino, P., Hot Melt Extrusion: Highlighting Physicochemical Factors to Be Investigated While Designing and Optimizing a Hot Melt Extrusion Process. *Pharmaceutics* **2018**, *10* (3), 89.
23. Martiel, I.; Sagalowicz, L.; Handschin, S.; Mezzenga, R., Facile Dispersion and Control of Internal Structure in Lyotropic Liquid Crystalline Particles by Auxiliary Solvent Evaporation. *Langmuir* **2014**, *30* (48), 14452-14459.
24. Kim, H.; Leal, C., Cuboplexes: Topologically Active siRNA Delivery. *Acs Nano* **2015**, *9* (10), 10214-26.
25. Zhang, H., Thin-Film Hydration Followed by Extrusion Method for Liposome Preparation. In *Liposomes: Methods and Protocols*, D'Souza, G. G. M., Ed. Springer New York: New York, NY, 2017; pp 17-22.
26. Kim, H.; Sung, J.; Chang, Y.; Alfeche, A.; Leal, C., Microfluidics Synthesis of Gene Silencing Cubosomes. *Acs Nano* **2018**, *12* (9), 9196-9205.
27. Yaghmur, A.; Ghazal, A.; Ghazal, R.; Dimaki, M.; Svendsen, W. E., A hydrodynamic flow focusing microfluidic device for the continuous production of hexosomes based on docosahexaenoic acid monoglyceride. *Phys. Chem. Chem. Phys.* **2019**, *21* (24), 13005-13013.
28. Hong, L.; Dong, Y.-D.; Boyd, B. J., Preparation of Nanostructured Lipid Drug Delivery Particles Using Microfluidic Mixing. *Pharm. Nanotechnol.* **2019**, *7* (6), 484-495.
29. Barriga, H. M. G.; Holme, M. N.; Stevens, M. M., Cubosomes: The Next Generation of Smart Lipid Nanoparticles? *Angew Chem Int Ed Engl* **2019**, *58* (10), 2958-2978.

30. Kulkarni, C. V.; Moinuddin, Z.; Agarwal, Y., Effect of fullerene on the dispersibility of nanostructured lipid particles and encapsulation in sterically stabilized emulsions. *J Colloid Interf Sci* **2016**, *480*, 69-75.
31. Angelova, M. I.; Dimitrov, D. S., Liposome Electroformation. *Faraday Discussions* **1986**, *81*, 303-311.
32. Pereno, V.; Carugo, D.; Bau, L.; Sezgin, E.; Bernardino de la Serna, J.; Eggeling, C.; Stride, E., Electroformation of Giant Unilamellar Vesicles on Stainless Steel Electrodes. *ACS omega* **2017**, *2* (3), 994-1002.
33. Kuribayashi, K.; Tresset, G.; Ph, C.; Fujita, H.; Takeuchi, S., Electroformation of giant liposomes in microfluidic channels. *Measurement Science and Technology* **2006**, *17* (12), 3121.
34. Drabik, D.; Doslak, J.; Przybylo, M., Effects of electroformation protocol parameters on quality of homogeneous GUV populations. *Chem Phys Lipids* **2018**, *212*, 88-95.
35. Herold, C.; Chwastek, G.; Schwille, P.; Petrov, E. P., Efficient Electroformation of Supergiant Unilamellar Vesicles Containing Cationic Lipids on ITO-Coated Electrodes. *Langmuir* **2012**, *28* (13), 5518-5521.
36. Bangham, A. D., Properties and uses of lipid vesicles: an overview. *Ann N Y Acad Sci* **1978**, *308*, 2-7.
37. Mezzenga, R.; Meyer, C.; Servais, C.; Romoscanu, A. I.; Sagalowicz, L.; Hayward, R. C., Shear Rheology of Lyotropic Liquid Crystals: A Case Study. *Langmuir* **2005**, *21* (8), 3322.
38. Barauskas, J.; Landh, T., Phase Behavior of the Phytantriol/Water System. *Langmuir* **2003**, *19* (23), 9562-9565.
39. Shalaev, E. Y.; Steponkus, P. L., Phase diagram of 1,2-dioleoylphosphatidylethanolamine (DOPE):water system at subzero temperatures and at low water contents. *Biochimica et Biophysica Acta (BBA) - Biomembranes* **1999**, *1419* (2), 229-247.
40. Ulrich, A. S.; Sami, M.; Watts, A., Hydration of DOPC bilayers by differential scanning calorimetry. *Biochimica et Biophysica Acta (BBA) - Biomembranes* **1994**, *1191* (1), 225-230.
41. Wanka, G.; Hoffmann, H.; Ulbricht, W., Phase Diagrams and Aggregation Behavior of Poly(oxyethylene)-Poly(oxypropylene)-Poly(oxyethylene) Triblock Copolymers in Aqueous Solutions. *Macromolecules* **1994**, *27* (15), 4145-4159.
42. Pérez-Fuentes, L.; Drummond, C.; Faraudo, J.; Bastos-González, D., Adsorption of Milk Proteins (β -Casein and β -Lactoglobulin) and BSA onto Hydrophobic Surfaces. *Materials* **2017**, *10* (8), 893.
43. Göpfrich, K.; Kulkarni, C. V.; Pambos, O. J.; Keyser, U. F., Lipid Nanobilayers to Host Biological Nanopores for DNA Translocations *Langmuir* **2013**, *29* (1), 355-364.
44. Sadeghpour, A.; Rappolt, M.; Misra, S.; Kulkarni, C. V., Bile Salts Caught in the Act: From Emulsification to Nanostructural Reorganization of Lipid Self-Assemblies. *Langmuir* **2018**, *34* (45), 13626-13637.
45. Barauskas, J.; Johnsson, M.; Tiberg, F., Self-Assembled Lipid Superstructures: Beyond Vesicles and Liposomes. *Nano Lett* **2005**, *5* (8), 1615-1619.
46. Kulkarni, C. V.; Vishwapathi, V. K.; Quarshie, A.; Moinuddin, Z.; Page, J.; Kendrekar, P.; Mashele, S. S., Self-Assembled Lipid Cubic Phase and Cubosomes for the Delivery of Aspirin as a Model Drug. *Langmuir* **2017**, *33* (38), 9907-9915.
47. Guillot, S.; Salentinig, S.; Chemelli, A.; Sagalowicz, L.; Leser, M. E.; Glatter, O., Influence of the Stabilizer Concentration on the Internal Liquid Crystalline Order and the Size of Oil-Loaded Monolinolein-Based Dispersions. *Langmuir* **2010**, *26* (9), 6222-6229.
48. Valldeperas, M.; Wiśniewska, M.; Ram-On, M.; Kesselman, E.; Danino, D.; Nylander, T.; Barauskas, J., Sponge Phases and Nanoparticle Dispersions in Aqueous Mixtures of Mono- and Diglycerides. *Langmuir* **2016**, *32* (34), 8650-8659.
49. Muller, F.; Salonen, A.; Glatter, O., Monoglyceride-based cubosomes stabilized by Laponite: Separating the effects of stabilizer, pH and temperature. *Colloids and Surfaces A: Physicochemical and Engineering Aspects* **2010**, *358* (1-3), 50-56.

50. López-Esparza, R.; Guedeau-Boudeville, M. A.; Larios-Rodríguez, E.; Maldonado, A.; Ober, R.; Urbach, W., Confinement of a hydrophilic polymer in membrane lyotropic phases. *Journal of Colloid and Interface Science* **2009**, *331* (1), 185-190.
51. Engström, S.; Alfons, K.; Rasmusson, M.; Ljusberg-Wahren, H., Solvent-induced sponge (L3) phases in the solvent-monoolein-water system. In *The Colloid Science of Lipids*, Lindmann, B.; Ninham, B. W., Eds. Steinkopff-Verlag Darmstadt.: 1998; pp 93-98.
52. Chen, Y.; Angelova, A.; Angelov, B.; Drechsler, M.; Garamus, V. M.; Willumeit-Romer, R.; Zou, A., Sterically stabilized spongosomes for multidrug delivery of anticancer nanomedicines. *Journal of Materials Chemistry B* **2015**, *3* (39), 7734-7744.
53. Angelov, B.; Angelova, A.; Mutaftchieva, R.; Lesieur, S.; Vainio, U.; Garamus, V. M.; Jensen, G. V.; Pedersen, J. S., SAXS investigation of a cubic to a sponge (L3) phase transition in self-assembled lipid nanocarriers. *Physical Chemistry Chemical Physics* **2011**, *13*, 3073-3081.
54. Angelov, B.; Angelova, A.; Drechsler, M.; Garamus, V. M.; Mutaftchieva, R.; Lesieur, S., Identification of large channels in cationic PEGylated cubosome nanoparticles by synchrotron radiation SAXS and Cryo-TEM imaging. *Soft Matter* **2015**, *11* (18), 3686-3692.
55. Siekmann, B.; Bunjes, H.; Koch, M. H.; Westesen, K., Preparation and structural investigations of colloidal dispersions prepared from cubic monoglyceride-water phases. *Int J Pharm* **2002**, *244* (1-2), 33-43.
56. Yagmur, A.; Laggner, P.; Almgren, M.; Rappolt, M., Self-assembly in monoelaidin aqueous dispersions: direct vesicles to cubosomes transition. *PLoS One* **2008**, *3* (11), e3747.
57. Kulkarni, C. V.; Tang, T. Y.; Seddon, A. M.; Seddon, J. M.; Ces, O.; Templer, R. H., Engineering Bicontinuous Cubic Structures at the Nanoscale– the Role of Chain Splay. *Soft Matter* **2010**, *6*, 3191-3194.
58. E. Shyamsunder, S. M. G., M. W. Tate, D. C. Turner, P. T. C. So, and C. P. S. Tilcock, Observation of inverted cubic phase in hydrated dioleoylphosphatidylethanolamine membranes. *Biochemistry* **1988**, *27* (7), 2332 - 2336.
59. Kurien, B. T.; Singh, A.; Matsumoto, H.; Scofield, R. H., Improving the Solubility and Pharmacological Efficacy of Curcumin by Heat Treatment. *ASSAY and Drug Development Technologies* **2007**, *5* (4), 567-576.
60. Stohs, S. J.; Chen, O.; Ray, S. D.; Ji, J.; Bucci, L. R.; Preuss, H. G., Highly Bioavailable Forms of Curcumin and Promising Avenues for Curcumin-Based Research and Application: A Review. *Molecules* **2020**, *25* (6), 1397.
61. Malheiros, B.; Dias de Castro, R.; Lotierzo, M. C. G.; Casadei, B. R.; Barbosa, L. R. S., Design and manufacturing of monodisperse and malleable phytantriol-based cubosomes for drug delivery applications. *Journal of Drug Delivery Science and Technology* **2021**, *61*, 102149.
62. Kulkarni, C. V., Hierarchically Structured Lipid Systems. In *Encyclopedia of Biophysics*, Roberts, G. C. K., Ed. Springer Berlin Heidelberg: Berlin, Heidelberg, 2013; pp 975-983.
63. Murgia, S.; Biffi, S.; Mezzenga, R., Recent advances of non-lamellar lyotropic liquid crystalline nanoparticles in nanomedicine. *Current Opinion in Colloid & Interface Science* **2020**, *48*, 28-39.
64. Zhai, J.; Fong, C.; Tran, N.; Drummond, C. J., Non-Lamellar Lyotropic Liquid Crystalline Lipid Nanoparticles for the Next Generation of Nanomedicine. *Acs Nano* **2019**, *13* (6), 6178-6206.
65. Angelova, A.; Garamus, V. M.; Angelov, B.; Tian, Z.; Li, Y.; Zou, A., Advances in structural design of lipid-based nanoparticle carriers for delivery of macromolecular drugs, phytochemicals and anti-tumor agents. *Advances in Colloid and Interface Science* **2017**, *249*, 331-345.
66. Younus, M.; Prentice, R. N.; Clarkson, A. N.; Boyd, B. J.; Rizwan, S. B., Incorporation of an endogenous neuromodulatory lipid, oleoylethanolamide, into cubosomes: nanostructural characterization. *Langmuir* **2016**, *32* (35), 8942–8950.
67. Barriga, H.; Ces, O.; Law, R. V.; Seddon, J. M.; Brooks, N. J., Engineering swollen cubosomes using cholesterol and anionic lipids. *Langmuir* **2019**, *35* (50), 16521–16527.